

# Numerical Solution of the Experimental Model: Traditional Approach Versus Optimization

**Mousa Salty Ababneh**

Department of Financial & Administrative Sciences  
Al-Balqa Applied University (BAU), Jordan

**Received** 2022 April 02; **Revised** 2022 May 20; **Accepted** 2022 June 18.

## **Abstract**

This paper proposes a near-Newton approach, using uni-dimensional Rossby-Obukhov and Korteweg-deVries (KdV) equations as models for the solution of the partial differential equations (PDE) -controlled problem. One extremely important aspect of the process is that the notation of differential equations does not restrict the stability of the step size. The traditional approach to solve regional models, the boundary conditions are obtained by interpolating the solution provided by the global model on the coarse mesh. Essentially, the global points within the regional domain are discarded. With the use of optimization tools we can reformulate the problem in order to take advantage of all available data. The intention of this work is to formulate an optimization problem that seeks to solve the model in such a way that the solution is as close as possible to the data contained in the domain, which can be interpreted as the interpolation of the data by solving the model equations. Currently, there is no theory to explain the stable behavior of the non-evolutionary problem. However, we can observe that the global data interpolated in the problem (weather forecast) act as a regularization, demanding that the solution does not deviate too far from the global data and does not present oscillatory behavior. In this paper it was present two comparative experiments using the experimental model to validate the above condition. The first experiment was done with the Rossby-Obukhov equation, and the second with the KdV equation. Just as each experiment comprises several numerical tests, we show only the most expressive results and comment on the behavior of others. It was illustrated that, the phenomenon in different linear problems (the heat equation and the Rossby-Obukhov equation) and nonlinear ones (the KdV equation), possible to obtain the solution of the problem with the speed compatible with a single direct evolution using usual PDE methods, without losing precision in the solution.

**Keywords:** PDF, KdV equation, Rossby-Obukhov equation, near-Newton approach, weather forecast, traditional approach versus optimization

---

## **1.0 Introduction**

A differential equation is an equation that relates a function of one or more variables with their derivatives [1-2]. The optimization technique used in the spatial model domain for Apkarian et al., (2020) [3] restores boundary conditions by means of data. The problem of regional weather forecasting means that the solution to the Cauchy-Dirichlet problem is particularly relevant in

weather. A distinction must be made between two types of predictive atmospheric models. There are global models that estimate the whole world and regional models that provide a prediction for a small area. The grid resolution is one of the fundamental variations between these models [4]. Low resolution space grids are used for global models and denser mesh regional models run. This is primarily a computational explanation for the presence of these two versions. Cauchy dirichlet problems also have to be solved by researching and modelling various physical processes. Numerical methods are typically used in geophysical studies to solve the Cauchy-Dirichlet problem [5]. Traditionally, these approaches use discrete types of equations and initial and limit values at grid points. Generally, the problem is solved with a valid numerical method. In the original and limits of measurements or other model outputs, though, all contain errors that can exceed 30 percent of the true values. The KKT (Karush Kuhn Tucker) non-linear mechanism [12] is well constructed in various optimization problems, and Newton and Quasi-Newton methods are very useful for its solution [6]. Our recommendation, implemented as part of meteorological data assimilation, enables the optimum solution of the model to be found with regard to the observed data at pace that is consistent with one single direct model growth [7]. This paper attempts to explain the actions of the experimental model using the equations Rossby-Obukhov and KdV. We implemented different schemes and studied their numerical behaviour for both equations. Then with the experimental model, we present some experiments. In this paper, the first trials of the Rossby Obukhov equation and the second of the KdV equations were conducted. Just when we present only the most expressive findings and comment on the behaviour of other approaches each experiment contains a variety of numerical experiments.

## **2.0 Numerical formulation of the regional problem: traditional approach**

In the specific case of the Cauchy-Dirichlet (C-D) problem for parabolic equations, the question about the existence and uniqueness of the solution is directly related to the structure of the boundary of its domain in the vicinity Lines of those points with horizontal tangent [11]. The C-D issue as described in the Regional Weather Forecasts is formulated here. We need the lateral boundary for the whole time interval needed to achieve a specific solution for regional model equations. These data are typically collected from a global model solution. We may not know the exact solution to the external model (if not our problem would have been solved), but we can find it in a discrete form.

### **2.1 Traditional approach**

In order to solve the regional model, it is necessary to define, in addition to the initial condition, the boundary condition at the boundary of specific domain for the entire period of time for which the forecast will be performed. The data for the contour are obtained from the global model, whose exact solution we do not know. We can, however, obtain the approximate solution of its discrete formulation:

$$\begin{aligned} \Delta_t \{\bar{\Psi}\} &= \bar{\mathcal{F}}_d \\ \bar{\Psi}(x, 0) &= \mathbb{Y}_{glob}(\bar{x}) \end{aligned} \text{..(Eq-1.1)}$$

When the evolutionary vector of world models is 't'  $\bar{\mathcal{F}}_d$  is a discrete vector, and the initial state is  $\mathbb{Y}_{glob}$   $\bar{\mathcal{F}}_d$  is a discrete external power. The numerical solution of (1.1), provided by the sun is believed to be adequate for the optimum hypothesis model, which represents the true main atmospheric processes exactly. It is believed that " $\bar{\Psi}_{Sol}$ " numerical (1.1) solution is fairly close to the optimal hypothesis model solution that precisely represents the actual large-scale atmospheric systems. The discrete representation of the regional model, defined in a closed area with a  $S$  border, can be written with,

$$\begin{aligned} \Delta_t &= \bar{\mathcal{F}}_{rd}; \\ \mathbb{G}(x, 0) &= \mathbb{Y}_{loc}(\bar{x}) \\ \mathbb{G}(\bar{x}, t) \Big|_{x \in S} &= \mathbb{G}_s(\bar{x}, t)..(Eq-1.2) \end{aligned}$$

' $\mathbb{G}$ ' is the vect or prognostic feature  $\bar{\mathcal{F}}_{rd}$  while ' $\Delta_t$ ' is the differential operator for the regional model's evolution; where the exterior characteristics are discrete, the original condition is ' $\mathbb{Y}_{loc}$ '. The traditional approach to solve (1.2) is to obtain the boundary condition  $\mathbb{G}_s$  by interpolating the necessary data from the global solution sol in the regional grid and then apply a numerical method to solve PDEs.

### 2.1.1 Experimental model

Real weather and climate forecasting models are complex PDE systems in relation to three-dimensional space. The spatial mesh for a regional model can contain on the order of  $400 \times 400 \times 100 = 16 * 10^6$  points and the number of steps in time, for a 4-day forecast, is on the order of  $4 * 10^3$ . Obviously, these values vary from one model to another, as they depend on many factors (numerical method for solving PDEs, type of mesh, type of discretization scheme, etc.). We present the values here only as a reference to illustrate the size of a real problem. The intention of this work is to approach the discrete problem of weather forecasting (1.2) or any other problem with these characteristics, as an inverse problem and to use the optimization tools to solve it. Our goal is to develop an efficient algorithm and study its behavior. For this purpose, we will use an experimental model that simulates the characteristics of real regional models, but with a simple physical description and a small numerical dimension. Below we characterize the model in detail:

**Physics:** the model is described only by a one-dimensional equation whose analytical solution is known.

**Discretization:** we adopt the finite difference method, which is often used in current models.

**Domain:** we take the model domain as a limited and closed area contained in the domain of the analytical solution.

**Global data:** we build global data using the analytical solution in a coarse mesh in space-time.

**Initial condition:** for our experimental model, we take the analytical solution as the initial condition in the initial instant of time.

We observed that the global data are obtained from the solution of the same equation that is used in the experimental model, while the real models, global and regional, and are described by different PDE systems. However, the fact of using only one equation to describe the model does not allow to simulate the same situation. In the case of the initial condition, obviously, it is not exact in reality, but it is obtained through a process, known as data assimilation, which

produces a good approximation of the state of atmosphere of the instant from which the model is executed. Therefore, the error related to the initial condition is significantly less than the error related to the global data. Just as our attention in this work is focused on the use of global data, we take the initial condition as being exact.

Next, we introduce the equations that will be used in our numerical tests with the experimental model.

## 2.2 One-dimensional Rossby-Obukhov equation

The Rossby-Obukhov equation was deduced by Obukhov in 1949 [8]. Its domain is a periodic  $\beta$ -plain, frequently used in theoretical studies of meteorology. A periodic  $\beta$ -plain is basically a cylinder, that is, a rectangle in which all solutions are periodic in  $x$ , with dimensions  $L = 3 \times 10^7$  m in the  $x$  direction and  $B = 4 \times 10^6$  m in the  $y$  direction. The Rossby-Obukhov equation is a potential vortices equation, which describes the evolution of the Rossby waves, responsible for the change in time. Its expression is given by

$$\frac{\partial}{\partial t} \left[ \nabla^2 \varphi - \frac{\varphi}{l_0^2} \right] + j(\varphi, \nabla^2 \varphi) + \beta \frac{\partial \varphi}{\partial x} = 0. \text{ (Eq - 1.3)}$$

where  $\varphi$  is the current function,  $f_o = 10^{-4} s^{-1}$  is the Coriolis parameter,  $C_o$  speed of sound,  $\beta = df_o / dt = 1.6 \times 10^{-11} s^{-1} s^{-1} m^{-1}$  and  $l_o = C_o / f_o = 3 \times 10^6$  m is to climb from Obukhov.

As with most non-linear PDEs, we do not know the general analytical solution to the Rossby-Obukhov equation. However, for the linearized one-dimensional case, given by

$$\frac{\partial}{\partial t} \left( \frac{\partial^2}{\partial x^2} - \frac{1}{l_0^2} \right) \varphi + \beta \frac{\partial \varphi}{\partial x} + U \frac{\partial^3 \varphi}{\partial x^3} = 0. \text{ (Eq - 1.4)}$$

the analytical solution is known.

## 2.3 Korteweg-de Vries equation

A dispersive nonlinear partial difference equation is the Korteweg-de Vries Equation. The mathematical model of the wave on the shallow surface of the water is given with equation 1.5:

$$u_t + 6uu_x + u_{xxx} = 0 \\ x \in \mathbb{R}, t > 0. \text{ (Eq - 1.5)}$$

Equation (1.5) has an analytical solution, as shown by Korteweg and de Vries [9], given by

$$u = b + a \operatorname{cn}^2(\gamma(x - V_t) | m). \text{ (Eq - 1.6)}$$

where  $\operatorname{cn}^2(\gamma(x - V_t) | m)$  is the Jacobian elliptic task,  $m \in (0, 1)$  is the unit of the elliptical function,  $\gamma$  is the wave number,  $a = 2m\gamma^2$  and  $V = 6b + 4(2m - 1)\gamma^2$ . This solution is called a cnoidal wave.

In the case where  $m \rightarrow 1$  we have  $\operatorname{cn}(x | m) \rightarrow \operatorname{sech}(x)$  and the solution (1.6) takes the form of a one-dimensional solid:

$$u = b + a \operatorname{sech}^2(\gamma(x - V_t)). \text{ (Eq - 1.7)}$$

with  $V = 6b + 2a$  and  $a = 2\gamma$ . Figure 1 shows the solution of the *KdV* equation at time  $t = 0$ .

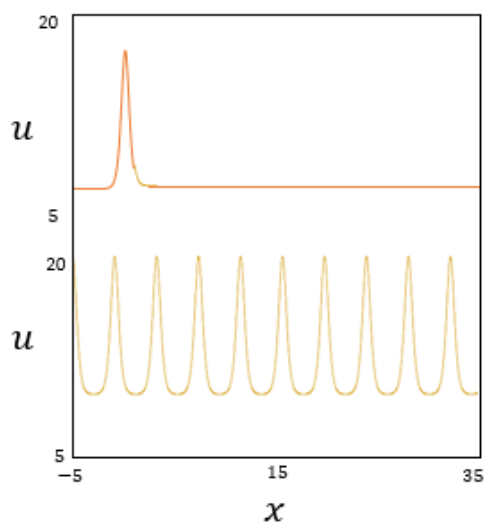


Figure 1: Graph of the solution of the KdV equation for  $t = 0$ : soliton with  $\gamma = 2$  and  $b = a$  (left); conical wave with  $\gamma = 2$ ,  $m = 0.995$  and  $b = a$  (on the right).

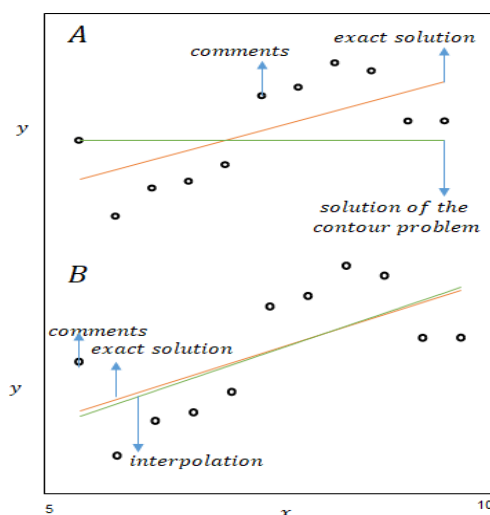


Figure 2: Solution of  $y'' = 0$ : contour problem (A) and interpolation by least squares (B).

As we described in the previous sections, in the traditional approach to solving regional models, the boundary conditions are obtained by interpolating the solution provided by the global model on the coarse mesh. Essentially, the global points within the regional domain are discarded. With the use of optimization tools we can reformulate the problem in order to take advantage of all available data.

Next, we'll look at a trivial example. Let  $y''' = 0$ , the "regional model", defined in  $[a, b]$  and  $\{(x_1 = a, y_1), \dots, (x_m = b, y_m)\}$ , the "global data" of the model. The classic approach is simply to take the solution as the line that joins  $(x_1, y_1)$  and  $(x_m, y_m)$ . However, instead, we can take as a solution a straight line that interpolates the points in the sense of minimum squares. If there are no errors in the data, all outcomes are the same. Although the variations may be important in the case of mistakes. In Figure 2 we demonstrate the illustration with the data  $(x_i, y_i + e_i), i = 1, \dots, m$ , extracted from the exact solution  $y = 2x + 1$ , where  $e_i$  corresponds to a random disturbance of  $y_i$  by up to 30%. It is easy to see that in this case the reasonable solution is the solution that interpolates the points.

The intention of this work is to formulate an optimization problem that seeks to solve the model in such a way that the solution is as close as possible to the data contained in the domain, which can be interpreted as the interpolation of the data by solving the model equations.

### 3.1 Formulation of the optimization problem

To formulate the optimization problem, let us consider a simple but very illustrative example, the supersensitive contour problem given by

$$\begin{aligned} \in x'' &= -xx' \\ x(0) &= -1, \\ x(1) &= 1 \dots (\text{Eq} - 1.8) \end{aligned}$$

The problem is called supersensitive, because small variations in the contour produce very different solutions, as we can see in Figure 3, where the value of  $x$  in 1 is between 0.998 and 1.002.

To obtain the analytical solution, we integrate the equation of the two sides

$$\epsilon \frac{x'}{x^2 + c} = -1/2 \dots \text{(Eq - 1.9)}$$

And integrating again, we have

$$x = \frac{\sqrt{-c} \left( 1 + \exp \frac{(t+k)\sqrt{-c}}{\epsilon} \right)}{1 - \exp \frac{(t+k)\sqrt{-c}}{\epsilon}} \quad \text{if } c \leq 0$$

$$\sqrt{c} \tan \left( \frac{(t+k)\sqrt{-c}}{\epsilon} \right), \text{ if } c > 0$$

Where constants  $c$  and  $K$  are defined by boundary conditions.

Suppose now that we want to solve equation (1.8) with the solution disturbed, at most 5%, at some points in the domain (Figure 4).

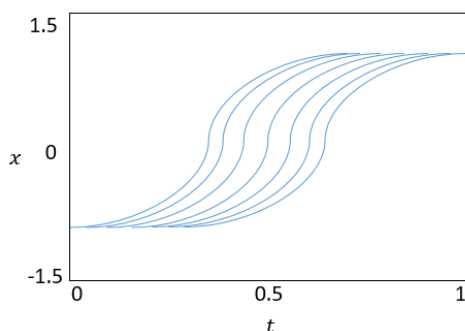


Figure 3: Analytical solution of  $\epsilon x'' = -xx'$ ,  $\epsilon = 0.05$  with  $x(0) = -1$  and  $x(1)$  varying close to 1.

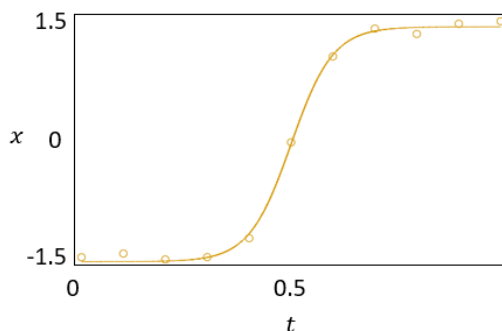


Figure 4: Solution of  $\epsilon x'' = -xx'$ ,  $\epsilon = 0.05$  with  $x(0) = -1$  and  $x(1) = 1$  and disturbed data.

Obviously, when trying to solve the problem numerically with an efficient method, using only the points on the contour, we obtain a solution far from the desired one, because the analytical solution for this disturbed contour is quite different. Figure 4 shows the numerical solution using the shooting method with 4-order Runge-Kutta discretization. So let's formulate the idea of looking for the solution that is as close as possible to the data. Let  $\{x_0 = 0, x_1, \dots, x_N = 1\}$  the mesh over the domain and suppose that is the vector of the discretization of equation (4.1) at the point of the mesh  $x_i$ ,  $i = 1, \dots, N - 1$ . With a simple example we saw that the use of data within the domain with an optimization formulation makes it possible to find the desired solution, while the contour problem (disturbed) provides a completely different solution. Therefore, we will apply the optimization to models that have these same characteristics, such as regional models in meteorology.

### 3.2 Regional modelling and optimization problem

Suppose we have a solution of (1.1) in a coarse (glob) mesh,  $\Psi_{Sol}$ . The objective is to find  $\mathbb{G}_{Sol}$  in the fine (regional) mesh that satisfies the regional model (1.2) and is as close as possible to the global sol  $\Psi_{Sol|s}$  solution. In terms of formulation (1.10),

Minimize  $d(x, \mathbb{V})$ ; *Subjected to*  $h(x) = 0..$ (Eq-1.10)

where  $d(.,.)$  is the distance.

The regional problem can be rewritten as

$$\begin{aligned} \text{Minimize } & \frac{1}{2} \|\mathbb{G} - \mathcal{F}(\Psi_{Sol} | s)\|_2^2 \\ & \Delta t \{\mathbb{G}\} - \mathcal{F}_{rd} = 0 \\ \mathbb{G}(0) - \mathbb{Y}_{loc}(x) &= 0.. \text{ (Eq - 1.11)} \end{aligned}$$

Basically, there are two ways to use the problem (1.11) to solve the regional model. The first is to apply it evolutionarily for each time level, that is, to do the procedure equivalent to that used in finite difference methods: given the initial condition at  $t_0$ , obtain the solution at  $t_1$  and then, considering the initial condition it is now given at  $t_1$ , obtaining the solution at  $t_2$  and so on.

The second way is to consider as the domain of the problem the mesh with all levels of time (until the end time). With that, all the information made available by the global model in the desired period will be used. In addition, as we will see below, for this “non-evolutionary” way of interpreting the problem, the space-time mesh can be considerably larger, preserving the same quality of solution and, most importantly, the stability criterion for the chosen scheme does not need to be satisfied.

Obviously, the disadvantage of considering the problem in the whole space-time domain is the size of the numerical problem when we want to obtain the solution for a long period of time. The way to limit the dimension of the problem is to divide the time domain into several blocks and solve the problem (1.12) for each block, considering the solution at the last time level of the previous block as the initial condition. The choice of the size of each block can depend on several factors: the size of the regional grid, the amount of global data, the type of discretization chosen, computational resources, among others.

#### 3.2.1 Algorithm

Note that the initial condition in the problem (1.4) can also be interpreted as a data, together with the global data, but of “better” quality. We rewrote the problem (1.4) in a generalized way as

$$\begin{aligned} \text{Minimize } & \frac{1}{2} \|u - V\|_P^2 \\ \text{Subjected to } & h(u) = 0 \\ & u \in \mathbb{R}^n \text{ (Eq - 1.12)} \end{aligned}$$

where  $P$  is a diagonal penalty matrix, which penalizes the “best” quality data, and  $h(u) = [h_1(u), h_2(u), \dots, h_m(u)]^T$  is the discretization vector regional equations at each point in the grid.

The  $n$  and  $m$  dimensions are, respectively, the number of stitches in the mesh and the number of discretizations. Note that  $n$  and  $m$  are related, because for each point of the mesh that is not in the contour or in the initial condition, there is a discretization. Writing the KKT conditions of the problem (1.13), we obtain a nonlinear system given by

$$\begin{aligned} P(u - V) + h'(u)^T \lambda &= 0 \\ h(u) &= 0 \dots \text{ (Eq - 1.13)} \end{aligned}$$

where  $\lambda$  is the vector of the Lagrange multipliers and  $h'(u)$  is the Jacobian matrix of the constraints

Considering the  $n + m$  dimension of the system (1.12), the methods that are efficient for their resolution are Newton and Quasi-Newton. With these observations, we will introduce the following Quasi-Newton algorithm to solve the problem (1.13).

### 3.2.1.1 Quasi-Newton algorithm

Given the penalty matrix  $P$ , the stopping criterion and the maximum number of iterations:

*Step 1. Initialization*

$$k = 0$$

$$\begin{pmatrix} u_0 \\ \lambda_0 \end{pmatrix} = \begin{pmatrix} V \\ 0 \end{pmatrix}$$

*Step 2. Solve the subproblem*

$$J(u_k, 0) \begin{pmatrix} \Delta u_0 \\ \Delta \lambda_0 \end{pmatrix} = - \begin{pmatrix} P(u_k - V) + h'(u_k)T\lambda \\ h(u_k) \end{pmatrix}$$

*Step 3. Update the point*

$$\begin{pmatrix} u_{k+1} \\ \lambda_{k+1} \end{pmatrix} = \begin{pmatrix} u_k \\ \lambda_k \end{pmatrix} + \begin{pmatrix} \Delta u_k \\ \Delta \lambda_k \end{pmatrix}$$

*Step 4. Check the stopping criterion*

*If the stopping criterion is not met, assign  $k = k + 1$  and return to step 2.*

### 3.3 Optimization and the stability criterion

We will now analyze the most interesting phenomenon that arises when the differential equation is solved using the optimization approach. The evolutionary result corresponds to the solution obtained in a traditional way, showing instability after a short period of time. On the other hand, in the non-evolutionary case, the solution always has a stable behavior. In addition, we can take a much longer step without losing the quality of the solution, where we purposely take  $a \frac{\Delta t}{\Delta x^2} = 400$  to show the robust behavior of the optimization method. The same phenomenon occurs with the time-centered and space-centered scheme, which is unconditionally unstable. Using the evolutionary form, the solution quickly becomes unstable, while the use of all levels of time allows to obtain the stable and accurate solution with much larger steps compared to the steps with traditional finite difference approach.

Currently, there is no theory to explain the stable behavior of the non-evolutionary problem. However, we can observe that the global data interpolated in the problem mesh act as a regularization, demanding that the solution does not deviate too far from the global data and does not show oscillatory behavior.

### 3.4 Discretization of the Rossby-Obukhov and KdV equations

The purpose of this section is to show the behavior of the experimental model using the Rossby-Obukhov and KdV equations. For that, we introduced schemes for the two equations and analyzed their numerical behavior. Then, we present tests with the experimental model.

#### 4.1 Discretization of the one-dimensional Rossby-Obukhov equation

Before proceeding with discretization, we note that for the numerical implementation of the one-dimensional Rossby-Obukhov equation (1.4) it is convenient to use the additional representation in order to avoid rounding problems. Taking scaling parameters as  $S = 6 \times 10^6 \text{ m}$ ,  $T = S / V = 6 \times 10^5 \text{ s}$ ,  $V = 10 \text{ m / s}$ , the dimensionless variables take the following form:

$$\tilde{x} = \frac{x}{S}; \tilde{t} = \frac{t}{T}; \tilde{\varphi} = \frac{T}{S^2} \varphi; \text{ Eq. (2.1)}$$

the dimensionless equation is given by



$$\frac{\partial}{\partial t} \left( \frac{\partial^2}{\partial \tilde{x}^2} - \frac{1}{b^2} \right) \tilde{\varphi} + \beta_0 \frac{\partial \tilde{\varphi}}{\partial \tilde{x}} + U_0 \frac{\partial^3 \tilde{\varphi}}{\partial \tilde{x}^3} = 0 \text{ Eq ..(2.2)}$$

Where

$$\frac{1}{b} = \frac{S}{l_0} = 2, \beta_0 = \frac{\beta S^2}{V} = 57.6 \text{ and } U_0 = \frac{U}{V} \in [0,3]$$

In the theoretical deductions and numerical results for the Rossby-Obukhov equation shown in this work, we will always use dimensional measures for greater convenience. However, it is important to note that the numerical implementation used the dimensionless form (2.1).

For notation abuse, we use the same letter to denote the PDE dependent variable and its discrete approximation, that is, we refer to  $\varphi^k$  as the  $\varphi(x_n, t_k)$  approximation. For numerical tests we consider the entire periodic spatial domain  $[0, L]$ , discretizing it with  $N + 1$  points,  $\{x_0 = 0, x_1, \dots, x_{N-1}, x_N = L\}$ . Therefore, the boundary condition is given by

$$\varphi_{0\pm 1}^k = \varphi_{N\pm 1}^k, k > 0, i = 0, \dots, N - 1 \text{ Eq ..(2.3)}$$

As an initial condition, we take the analytical solution (1.6) at time  $t = 0$ , that is,

$$\varphi_n^0 = \sum_{i=1}^{85} A_i \text{Sen} [k_i x_n + \phi_i] \quad n \in \{0, \dots, N - 1\}$$

with the coefficients  $A_i$  and  $\phi_i$  generated randomly between  $[0, 10]$  and  $[0, 2\pi]$ , respectively.

## 4.2 Discretization of the KdV equation

Next, we introduce three finite difference schemes for the Korteweg-de Vries equation. We will not do the theoretical analysis of stability, since, being the non-linear equation, it is a complex procedure and is not the objective of this work (there are many publications that present a detailed analysis of stability for various KdV schemes).

For the numerical tests, we consider the interval  $[-5, 35]$  as the spatial domain, discretizing it with  $N + 1$  points,  $\{x_0 = -5, x_1, \dots, x_{N-1}, x_N = 35\}$ . For the initial and boundary conditions we use the two analytical solutions shown in Figure 1 - cnoidal solution, with  $m = 0.995$ , and soliton solution. The coefficients are  $\gamma = 2$  and  $b = a$ .

### 4.2.1 Explicit linear scheme

We set up the first scheme using the same idea as the time-centered and space-centered scheme of the Rossby-Obukhov equation.

$$\frac{u_n^{k+1} - u_n^{k-1}}{2\Delta t} + 6u_n^k \frac{u_{n+1}^k - u_{n-1}^k}{2\Delta x} + \frac{u_{n+2}^k - 2u_{n+1}^k + 2u_{n-1}^k - u_{n-2}^k}{2\Delta x^3} \text{ Eq ..(2.4)}$$

In Figure 5 we can see the solution for the soliton and cnoidal wave at time  $t = 0.5$ , with steps in space  $\Delta x = 0.05$  and  $\Delta x = 0.02$  (the step in time is the maximum allowed).

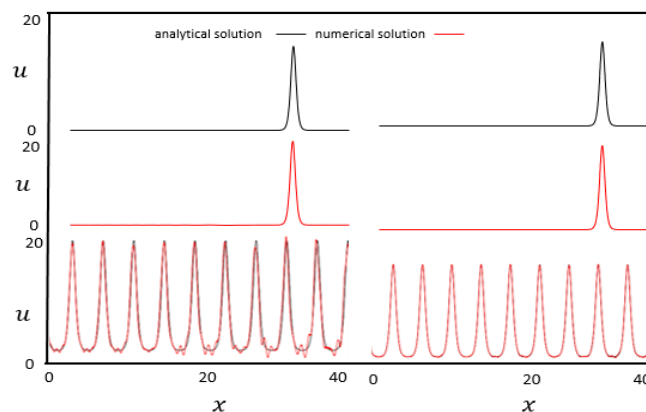


Figure 5: Numerical solutions of the KdV equation at time  $t = 0.5$  with  $\Delta x = 0.05$ ,  $\Delta t = 5 \times 10^{-5}$  (above) and  $\Delta x = 0.02$ ,  $\Delta t = 3.1 \times 10^{-6}$  (below). Explicit linear scheme.

#### 4.2.2 Implicit linear scheme

The second scheme is basically the Crank-Nicolson scheme. The difference is that, to preserve the linearity of the scheme in relation to  $u_{k+1}$  in the nonlinear term  $6u_x u$ ,  $u$  is discretized at the time level  $k$ . The resulting scheme, which we call the implicit linear scheme, is given by

$$\frac{u_n^{k+1} - u_n^{k-1}}{\Delta t} + 6u_n^k \frac{1}{2} \left( \frac{u_{n+1}^{k+1} - u_{n-1}^{k+1}}{2\Delta x} + \frac{u_{n+1}^k - u_{n-1}^k}{2\Delta x} \right) + \frac{1}{2} \left( \frac{u_{n+2}^k - 2u_{n+1}^{k+1} + 2u_{n-1}^{k+1} - u_{n-2}^{k+1}}{2\Delta x^3} + \frac{u_{n+2}^k - 2u_{n+1}^k + 2u_{n-1}^k - u_{n-2}^k}{2\Delta x^3} \right) = 0 \text{ Eq. (2.5)}$$

#### 4.2.3 Implicit nonlinear scheme

As a last scheme, which we call the implicit non-linear scheme, we will take the scheme deduced by Furihata in [10] and which satisfies the mass and energy conservation properties:

$$\begin{aligned} \frac{u_n^{k+1} - u_n^k}{\Delta t} + \frac{1}{2\Delta x} & \left( (u_{n+1}^{k+1})^2 + (u_{n-1}^{k+1})^2 + u_{n+1}^{k+1}u_{n+1}^k - u_{n-1}^{k+1}u_{n-1}^k + (u_{n+1}^k)^2 - (u_{n-1}^k)^2 \right) \\ & + \frac{1}{2\Delta x^3} \left( \frac{u_{n+2}^{k+1} + u_{n+2}^k}{2} - (u_{n+1}^{k+1} + u_{n+1}^k) + (u_{n-1}^{k+1} + u_{n-1}^k) - \frac{u_{n-2}^{k+1} + u_{n-2}^k}{2} \right) \\ & = 0 \text{ Eq. (2.6)} \end{aligned}$$

Figure 6 shows the numerical results obtained with the time step  $\Delta t = 2 \times 10^{-2}$ . With the  $10^{-10}$  stop criterion, Newton's method converged in 4 steps at each time level. We conclude this section by observing that for the KdV equation to be solved with reasonable precision, a very fine spatial grid is required, in addition to a very small relationship between the steps in time and space (the best relationship shown in the graphs is the nonlinear scheme, being  $10^{-2}$  for the period of evolution in the time of 0.5).

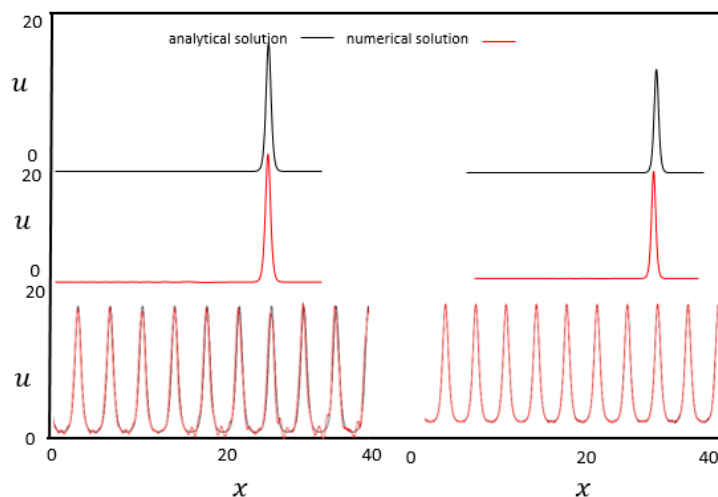


Figure 6: Numerical solutions of the KdV equation at time  $t = 0.5$  with  $\Delta t = 2 \times 10^{-4}$  and  $\Delta x = 0.05$  (above),  $\Delta x = 0.02$  (below). Implicit nonlinear scheme.

In this chapter we present three comparative experiments using the experimental model to validate the proposal presented in the previous sections

**5.0 Rossby-Obukhov equation**

First, we analyze the behavior of the experimental model with the Rossby-Obukhov equation. We consider as the regional domain the interval  $\{1.8 \times 10^7, 2.4 \times 10^7\}$ m (**6000 km in length**) within the periodic domain  $[0, L]$ .

To form the initial condition we use the analytical solution given by  $\varphi(x, t) = \sum_{i=1}^{K=85} A_i \text{Sen}[k_i x_n + \phi_i] \epsilon\{1.8 \times 10^7, 2.4 \times 10^7\}$  (Eq. 3.1)

The 85 harmonics, defined by the  $A_i$  and  $A_{ii}$  coefficients, correspond to the solution shown in Figure 2 and are the same as those used in tests with the Rossby-Obukhov equation in previous section We will take the speed as  $U = 30 \text{ m / s}$ .

**5.1. Experiment 1**

Global data: We will generate the global data as follows:

$$\frac{\Delta x_{global} \quad \Delta t_{global}}{300 \text{ km} \quad 2 \text{ hours}}$$

- we chose the global grid as:  $\Delta x_{global} \quad \Delta t_{global} \quad 300 \text{ km} \quad 2 \text{ hours}$  for the spatial domain  $[0, L]$  and temporal domain  $[0, 96]$  hours.
- on the mesh we generate the analytical solution with 85 harmonics;
- we consider the generated solution as the global data (shown in 7).

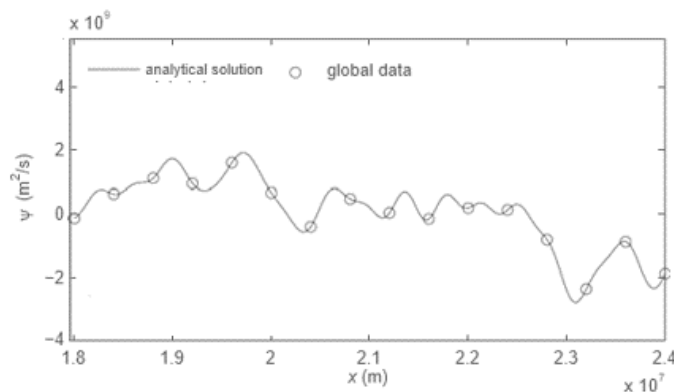


Figure 7: EXPERIMENT 1. Global data for the Rossby-Obukhov equation at  $t = 0$ .

**5.1.1 Boundary condition:** We generate the boundary condition simply by linearly interpolating the global data in the mesh of the experimental model.

First, we solve the experimental model using the traditional approach. We chose only two schemes - time-centered and space-centered, and Crank-Nicolson, - which showed the best behavior when resolved with an exact outline (presented in the previous chapter). The steps in time and space for each scheme were chosen as large as possible, but in such a way that the reduction in steps does not show significant variation in the solution of the problem. In Figures 8 and 9 we can see the graphs of the solution at time  $t = 24, 48$  and  $96$  hours, for the present schemes.

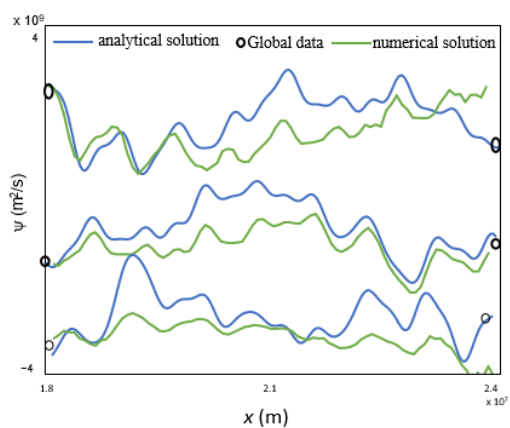


Figure 8: Experiment 1. Traditional Approach. Scheme centered in time and centered in space. Mesh:  $\Delta x = 10$  km,  $\Delta t = 333$  s. Solution at time  $t = 24$  hours (first graph),  $t = 48$  hours (second) and  $t = 96$  hours (third). CPU time = 0.13 s.

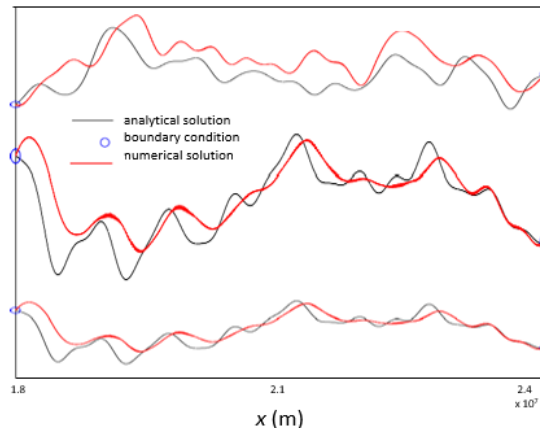


Figure 9: Experiment 1. traditional approach. Crank-Nicolson scheme. Mesh:  $\Delta x = 10$  km,  $\Delta t = 200$  s. Solution at time  $t = 24$  hours (first graph),  $t = 48$  hours (second) and  $t = 96$  hours (third). CPU time = 0.44 s.

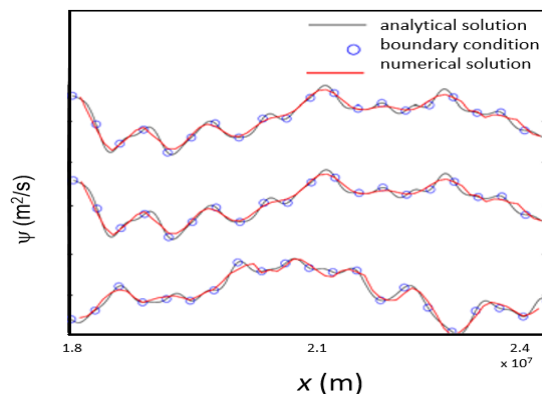


Figure 10: EXPERIMENT 1. OPTIMIZATION APPROACH. Scheme centered in time and centered in space. Mesh:  $\Delta x = 100$  km,  $\Delta t = 3600$  s. Solution at time  $t = 24$  hours (first graph),  $t = 48$  hours (second) and  $t = 96$  hours (third). CPU time = 0.63 s.

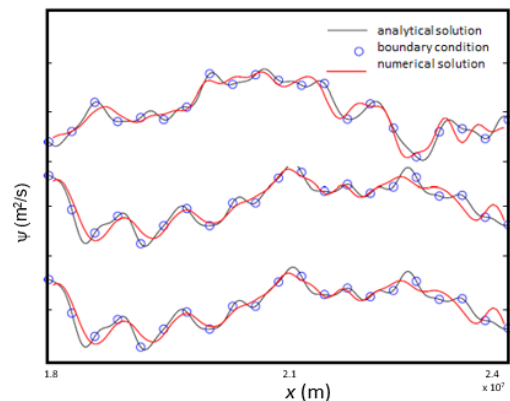


Figure 11: EXPERIMENT 1. OPTIMIZATION APPROACH. Crank-Nicolson scheme. Mesh:  $\Delta x = 50$  km,  $\Delta t = 1800$  s. Solution at time  $t = 24$  hours (first graph),  $t = 48$  hours (second) and  $t = 96$  hours (third). CPU time = 2.9 s.

We can see that due to the errors in the contour caused by the linear interpolation of the global data, the solution of the experimental model diverges in a short time from the analytical solution, that is, when there is no more influence from the initial condition. And the greater the errors in the contour, the worse the solution of the model will be.

Now we are going to solve the experimental model using the optimization approach, with the same schemes. The steps in space and time were chosen to be the largest possible. The penalty for the initial condition is  $10^4$ , that is, we take the penalty matrix  $I$  is the identity matrix.

We observed that the solution obtained by the optimization problem using the time-centered and space-centered scheme shown in Figure 10 &, despite the steps violating the stability condition (5.12), presents a very good behavior. And we can also note that in order to reach the acceptable precision in the solution by optimization, the steps in time and space are significantly greater than those necessary for the traditional solution with exact contour. In this first experiment we show that small errors in the boundary

condition can lead to strong distortions in the solution. However, the use of the optimization method with the data inside the domain provides a way to avoid the sensitivity of the solution to errors in the contour, allowing to obtain a good solution. We want to generate more realistic global data, that is, without containing information on small scales. For that, we take the analytical solution with only 25 harmonics and, from this solution, we generate the global data in the same mesh as the previous test, as shown in Figure 11. Thus, the smallest wave size present in the global data is 1200 km.

**5.2 Korteweg-de Vries:** We have already seen that in the case of the Rossby-Obukhov equation, which is a linear equation, errors in the contour propagate quickly into the domain, significantly distorting the solution. In this section we show the behavior of the non-linear KdV equation. We carried out the tests with the two solutions presented in the previous section: cnoidal wave and only soliton. Since the soliton is a single wave, while the cnoidal solution describes infinite waves, we take different domains for the two solutions. In the case of soliton, we obviously want to visualize the solution in the domain where the wave is present, so we chose the large spatial domain and as a temporal domain we took enough time for the wave to travel through the spatial domain. In the case of a cnoidal solution, unlike soliton, we analyze the behavior over a long period of time, but in the small spatial domain.

To generate the initial conditions and global data we use the analytical solutions (3.10) (cnoidal wave), with  $m = 0.995$ , and (3.11) (soliton), using the coefficients  $a = b$  and  $\gamma = 2$ .

### 5.2.1 Experiment 2

We present the first tests with the cnoidal solution of the KdV equation. As a domain we will take the interval  $[0, 10]$  in space and  $[0, 5]$  in time.

**Global data:** Using the same idea as in experiment 1, we generate the data from the analytical solution in a mesh given by

$$\begin{array}{cc} \Delta x_{global} & \Delta t_{global} \\ 0.5 & 0.005 \end{array}$$

and disturb the result by up to 10%,.

In the numerical resolution of the experimental model by the traditional approach, using only the contour, the disturbances from the global data make it impossible to obtain an acceptable solution of the equation even for a very short period of time, regardless of the chosen scheme. For the implicit nonlinear scheme, which showed the best behavior in the solution with exact contour, we can see in Figure 6.14, that the oscillations at time  $t = 0.1$  are already significant, and at  $t = 5$  the numerical solution is completely chaotic. It is important to note that in the same mesh,  $\Delta x = 0.02$  and  $\Delta t = 0.0002$ , the exact contoured solution is very close to the analytical solution. Applying the optimization approach and using the penalty matrix (6.2) of experiment 1, the best result is obtained by the implicit non-linear scheme in the mesh with  $\Delta x = 0.2$  and  $\Delta t = 0.005$ . Note that the mesh is much thicker than in the case of the solution by the traditional approach, but it was still necessary to divide the problem domain into blocks, each with a time size equal to 1, which makes it possible to control the size of the numerical problem and, hence, computer memory. The advantage of the optimization method is evident. In addition to obtaining the solution, the time spent by the CPU to solve the optimization problem is significantly less. This is due to the dimension of the problem, which in the case of optimization is at least 250 times smaller, in addition to the use of a block solution. Finally, we performed the tests with soliton. We chose the  $[-5, 35]$  interval as the spatial domain and, consequently, the time interval in which the soliton traverses the spatial domain is  $[0, 0.5]$ . The global data at time  $t = 0$ . Applying the traditional approach with implicit nonlinear scheme, using the same steps in space and time as in the previous test with the cnoidal wave, that the results show the increasing oscillations introduced by the errors in the boundary, while optimization solution is regularized by global data and does not present

significant errors. Experiment 2 clearly shows that the optimization approach makes it possible to obtain the solution that is not affected by random errors present in the data. Using the block solution it is possible to evolve the model for any period of time, as shown by the tests with the cnoidal wave. The choice of block size depends on the computational potential, for a powerful computer with a large amount of memory, it is possible to increase the time interval of each block, making more use of the information provided by the global model or by the measurements. The block size also determines the speed of convergence of the optimization problem. And its optimal size depends on several factors, such as computer configuration, quality of implementation, programming language used, among others.

## 6.0 Conclusion

In this study we construct the combined task of getting the solution to the global prototype and data assimilation as a partial differential equations. The results of the numerical tests presented here demonstrate that the optimization method will considerably increase the accuracy of the data solution pursued by the regional model if there are errors in the boundary values, but there are details about the efficiency of the requested solution in many internal points. Even where the problem of Cauchy-Dirichlet is vulnerable to border problems, the optimization approach helps you to create a solution that is similar to the analytical solution. In other situations, the solution is more sensitive. We have performed experiments with nonlinear Rossby-Oboukhov two-dimensional equations. The preliminary findings also show the substantial progress of the digital solution of the boundary problem with border value errors using the optimization technique. The problem of minimizing  $\|u - u_{data}\|^2$  subject to  $Au = b$  is only poorly conditioned if all the square submatrices are poorly conditioned. This explains why, in our case, we never encounter mal-conditioning and we can always work with schemes that, from the point of view of Cauchy's classic problem, are unstable. In the thesis we illustrated this phenomenon in different linear problems (the heat equation and the Rossby-Obukhov equation) and nonlinear ones (the KdV equation), so that it was possible to obtain the solution of the problem with the speed compatible with a single direct evolution using usual methods in PDE, without losing precision in the solution.

## References

1. Evans, L.C., Partial Differential Equations, Graduate Studies in Mathematics, 19, American Mathematical Society, Providence, RI, 1998.
2. John, F., Partial Differential Equations, Fourth edition, Applied Mathematical Sciences 1, Springer-Verlag, New York, 1982.
3. Apkarian, Pierre & Noll, Dominikus. (2020). Boundary control of partial differential equations using frequency domain optimization techniques. *Systems & Control Letters*. 135. 104577. 10.1016/j.sysconle.2019.104577.
4. Gunzburger, M. & Lee, Jeehyun. (2000). Domain decomposition method for optimization problems for partial differential equations. *Computers & Mathematics With Applications - COMPUT MATH APPL*. 40. 177-192. 10.1016/S0898-1221(00)00152-8.
5. Rubio, Gerardo. (2011). The Cauchy-Dirichlet Problem for a Class of Linear Parabolic Differential Equations with Unbounded Coefficients in an Unbounded Domain. *International Journal of Stochastic Analysis*. 2011. 10.1155/2011/469806.
6. Mitake, Hiroyoshi. (2008). The large-time behavior of solutions of the Cauchy-Dirichlet problem for Hamilton-Jacobi equations. *Nonlinear Differential Equations and Applications NoDEA*. 15. 347-362. 10.1007/s00030-008-7043-y.

7. Khiyabani, Farzin & Leong, Wah. (2014). Quasi-Newton methods based on ordinary differential equation approach for unconstrained nonlinear optimization. *Applied Mathematics and Computation*. 233. 272–291. 10.1016/j.amc.2014.01.171.
8. Hovhannisyanyan, Gro. (1988). On weighted Cauchy and Dirichlet problems for certain partial differential equations singular on the boundary. *Izv. AN Arm. SSR, Matematika*, [English translation: *Soviet Journal of Contemporary Math. Analysis - (Armenian Academy of Sciences)*]. 23. 3-21.
9. Campbell, L. & Maslowe, Sherwin. (2001). A numerical simulation of the nonlinear critical layer evolution of a forced Rossby wave packet in a zonal shear flow. *Mathematics and Computers in Simulation*. 55. 365-375. 10.1016/S0378-4754(00)00293-7.
10. Ma, Wen-Xiu & You, Yuncheng. (2005). Solving the Korteweg-de Vries Equation by Its Bilinear Form: Wronskian Solutions. *Transactions of the American Mathematical Society*. 357. 10.2307/3845133.
11. Cao, Wanrong & Zeng, Fanhai & Zang, Handy & Karniadakis, George. (2016). Implicit-Explicit Difference Schemes for Nonlinear Fractional Differential Equations with Nonsmooth Solutions. *SIAM Journal on Scientific Computing*. 38. 10.1137/16M1070323.
12. Figueroa Medina, Alberto & Tarko, Andrew. (2007). Speed Changes in the Vicinity of Horizontal Curves on Two-Lane Rural Roads. *Journal of Transportation Engineering-asce - J TRANSP ENG-ASCE*. 133. 10.1061/(ASCE)0733-947X(2007)133:4(215).
13. Wang, Yun & Zhang, L.W.. (2009). Properties of equation reformulation of the Karush–Kuhn–Tucker condition for nonlinear second order cone optimization problems. *Mathematical Methods of Operations Research*. 70. 195-218. 10.1007/s00186-008-0241-x.